

Pressure and non-linear susceptibilities in QCD at finite chemical potentials

Rajiv V. Gavai* and Sourendu Gupta†

*Department of Theoretical Physics, Tata Institute of Fundamental Research,
Homi Bhabha Road, Mumbai 400005, India.*

Abstract

When the free energy density of QCD is expanded in a Taylor series in the chemical potential, μ , the coefficients are the non-linear quark number susceptibilities. We show that these depend on the prescription for putting chemical potential on the lattice, making all extrapolations in chemical potential prescription dependent at finite lattice spacing. To put bounds on the prescription dependence, we investigate the magnitude of the non-linear susceptibilities over a range of temperature, T , in QCD with two degenerate flavours of light dynamical quarks at lattice spacing $1/4T$. The prescription dependence is removed in quenched QCD through a continuum extrapolation, and the dependence of the pressure, P , on μ is obtained.

PACS numbers: 11.15.Ha, 12.38.Gc

TIFR/TH/03-07, hep-lat/0303013

*Electronic address: gavai@tifr.res.in

†Electronic address: sgupta@tifr.res.in

One of the most important objects in the study of hot and dense hadronic matter is the phase diagram, particularly, the location of the critical end point, characterised by the temperature T_E and the chemical potential μ_E . Much effort has been expended recently on estimating these quantities at finite lattice spacing, a , using, implicitly [1] or explicitly [2, 3, 4], a Taylor series expansion of the free energy density. This needs the non-linear susceptibilities which define the response to an applied μ beyond quadratic order. An equally important question for phenomenology arises from the fact that present day heavy-ion collision experiments access the part of the QCD phase diagram with $\mu \simeq 10\text{--}80$ MeV, *i.e.*, baryon chemical potential $\mu_B \simeq 30\text{--}250$ MeV [5], far from μ_E . It is then pertinent to ask how relevant the $\mu = 0$ lattice QCD computations of quantities such as the pressure, P , are to these experiments.

In this paper we present the first investigation of these non-linear susceptibilities. We uncover essential lattice artifacts, but manage to quantify and remove them in the process of taking the continuum limit. We explicitly construct a Taylor series expansion for P at $\mu > 0$, put limits on the region of linear response, *i.e.*, of reliable extrapolations, and show that the $\mu = 0$ lattice computations are clearly relevant to experiments. An interesting sidelight is that there is strong evidence of short thermalisation times in the dense matter formed in these heavy-ion collisions [6], which may be related to large values of transport coefficients [7]. Most computations of such dynamical quantities are based on linear response theory. The success of the linear approximation in static quantities at fairly large driving also gives us confidence in using linear response theory for dynamics. Another interesting point is that the radius of convergence of a Taylor series expansion started near T_c [8] must give information on the location of the critical end-point, (T_E, μ_E) , through the Taylor coefficients, *i.e.*, the non-linear susceptibilities. Since these Taylor coefficients turn out to be prescription dependent and subject to strong finite lattice spacing effects, it seems that present day estimates of the end point will have to be sharpened strongly before they can be used as a guide to phenomenology.

The partition function of QCD at finite temperature T and chemical potentials μ_f for each flavour f can be written as

$$Z \equiv e^{-F/T} = \int \mathcal{D}U e^{-S(T)} \prod_f \text{Det } M(m_f, T, \mu_f). \quad (1)$$

F is the free energy, S is the gluon part of the action, M is the Dirac operator, each

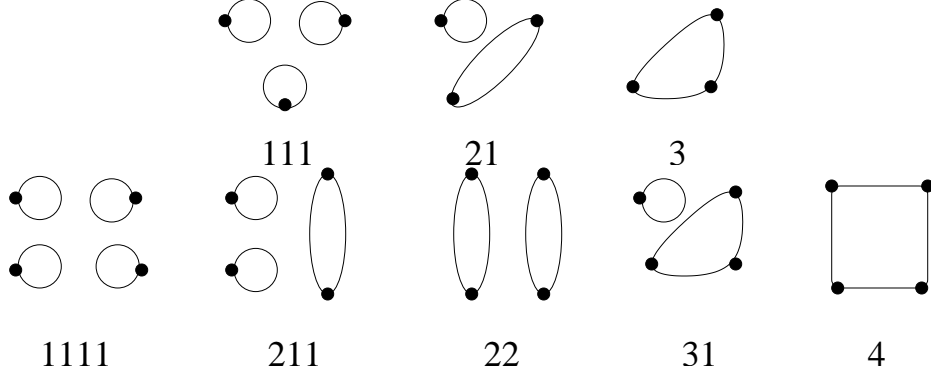


FIG. 1: All topologies which contribute to derivatives up to fourth order, and the notation for the corresponding operators.

determinant is for one quark flavour and the temperature T enters through the shape of the lattice and boundary conditions [9]. We shall work with a lattice discretisation and use staggered quarks [10]. In this work we shall only consider two degenerate flavours of quarks— $m_u = m_d = m$ [11], with chemical potentials μ_u and μ_d . The number densities, n_f , and the (linear) quark number susceptibilities, χ_{fg} , are the first and second derivatives of $-F/V$ with respect to μ_f and μ_g [12]. Since $P = -F/V$ for a homogeneous system, the non-linear susceptibilities of order $n \geq 3$ are also the remaining Taylor coefficients of an expansion of P —

$$\chi_{fg\dots} = -\frac{1}{V} \frac{\partial^n F}{\partial \mu_f \partial \mu_g \dots} = \frac{T}{V} \frac{\partial^n \log Z}{\partial \mu_f \partial \mu_g \dots}, \quad (2)$$

where we construct the expansion around $\mu_f = 0$.

We now write systematic rules for the construction of the non-linear susceptibilities. The derivatives of $\log Z$ needed in eq. (2) can be related to the derivatives of Z with respect to the chemical potentials μ_f , μ_g , *etc.*, (which we denote by $Z_{fg\dots}$) by the usual formulæ for taking connected parts [13]. The only extra point to remember is that all the odd derivatives vanish by CP symmetry. To write the subsequent formulæ compactly, we define operators \mathcal{O}_i by

$$Z_f = Z \langle \mathcal{O}_1 \rangle, \quad \text{and} \quad \mathcal{O}_{n+1} = \frac{\partial \mathcal{O}_n}{\partial \mu_f}, \quad (3)$$

where angular brackets denote averages over the ensemble defined by eq. (1) at $\mu_f = 0$. Diagrammatic rules [14] for the \mathcal{O}_i and the derivatives of Z , are—

1. Put down n vertices (each corresponding to a derivative of M with respect to μ_f) and label each with its flavour index.

2. Join the vertices by lines (each representing a quark) into sets of closed loops such that each loop contains only vertices of a single flavour. \mathcal{O}_i is denoted by a single loop joining i vertices.
3. For degenerate flavours and $\mu_f = 0$, the operators are labeled only by the topology, which is specified completely by the number of vertices per loop and the number of such loops. Therefore erase the flavour index after step 2. We denote each resulting operator by the notation $\mathcal{O}_{ij\dots} = \mathcal{O}_i\mathcal{O}_j\dots$, where $i + j + \dots = n$.
4. For each n -th order derivative of Z , add all the operator topologies for fixed n with flavour-dependent multiplicity equal to the number of ways in which each topology arises given the flavour indices.

The number densities $n_u = n_d = (T/V)\langle\mathcal{O}_1\rangle$ vanish at $\mu = 0$. We have considered the (linear) susceptibilities $\chi_3 = (T/V)\langle\mathcal{O}_2\rangle$ and $\chi_{ud} = (T/V)\langle\mathcal{O}_{11}\rangle$ extensively in a recent series of papers [21]. The new quantities that we now consider are the two third order derivatives

$$Z_{uuu} = Z\langle\mathcal{O}_3 + 3\mathcal{O}_{12} + \mathcal{O}_{111}\rangle \quad \text{and} \quad Z_{uud} = Z\langle\mathcal{O}_{12} + \mathcal{O}_{111}\rangle, \quad (4)$$

the three fourth order derivatives

$$\begin{aligned} Z_{uuuu} &= Z\langle\mathcal{O}_4 + 4\mathcal{O}_{13} + 3\mathcal{O}_{22} + 6\mathcal{O}_{112} + \mathcal{O}_{1111}\rangle, \\ Z_{uuud} &= Z\langle\mathcal{O}_{13} + 3\mathcal{O}_{112} + \mathcal{O}_{1111}\rangle, \\ Z_{uudd} &= Z\langle\mathcal{O}_{22} + 2\mathcal{O}_{112} + \mathcal{O}_{1111}\rangle, \end{aligned} \quad (5)$$

and the five corresponding susceptibilities. The third order susceptibilities turn out to vanish. The fourth order susceptibilities are

$$\begin{aligned} \chi_{uuuu} &= \left(\frac{T}{V}\right) \left[\frac{Z_{uuuu}}{Z} - 3 \left(\frac{Z_{uu}}{Z}\right)^2 \right], \\ \chi_{uuud} &= \left(\frac{T}{V}\right) \left[\frac{Z_{uuud}}{Z} - 3 \left(\frac{Z_{uu}}{Z}\right) \left(\frac{Z_{ud}}{Z}\right) \right], \\ \chi_{uudd} &= \left(\frac{T}{V}\right) \left[\frac{Z_{uudd}}{Z} - \left(\frac{Z_{uu}}{Z}\right)^2 - 2 \left(\frac{Z_{ud}}{Z}\right)^2 \right]. \end{aligned} \quad (6)$$

The operators contributing to eqs. (4, 5) are shown in Figure 1. Note the interesting fact that beyond the second order, the number of distinct operator topologies is greater than the

number of susceptibilities [14]; however by making N_f sufficiently large, all topologies up to any given order can be given a physical meaning.

A perturbative expansion in the continuum proceeds through an order-by-order enumeration of interaction terms. In the continuum the diagrams in Figure 1 are the leading order (ideal quark gas) part of the perturbative expansion of the susceptibilities, where each vertex corresponds to the insertion of a γ_0 (since the chemical potential enters the Lagrangian as $\gamma_0\mu_f$). Higher order Feynman diagrams correspond to dressing these loops by gluon attachments in all possible ways.

In the lattice theory the diagrams in Figure 1 stand for operator definitions which need further specification. They are not Feynman diagrams, but mnemonics for the process of taking derivatives of Z . Since, the coupling of Fermions to the chemical potential is non-linear [15], hence all derivatives of M exist and are non-zero in general. Using the identity $\text{Det } M = \exp(\text{Tr } \ln M)$ it is easy to get the usual expression $\mathcal{O}_1 = \text{Tr } M^{-1}M'$, where M' is the first derivative of M with respect to a chemical potential. Next, using the chain rule

$$\frac{dM^{-1}}{d\mu_f} = -M^{-1}M'M^{-1}, \quad (7)$$

which comes from the identity $MM^{-1} = 1$, we recover the relation $\mathcal{O}_2 = \text{Tr}(-M^{-1}M'M^{-1}M' + M^{-1}M'')$, where M'' is the second derivative of M with respect to the chemical potential. Higher operators can be derived by repeated application of the chain rule with eq. (7), and involve higher derivatives of M , which we write as $M^{(n)}$ (a systematic method for doing this is given in the appendix). In particular,

$$\begin{aligned} \mathcal{O}_3 &= \text{Tr} \left[2(M^{-1}M')^3 - 3M^{-1}M''M^{-1}M' + M^{-1}M^{(3)} \right] \\ \mathcal{O}_4 &= \text{Tr} \left[-6(M^{-1}M')^4 - 3(M^{-1}M'')^2 + 12M^{-1}M''(M^{-1}M')^2 \right. \\ &\quad \left. - 4M^{-1}M^{(3)}M^{-1}M' + M^{-1}M^{(4)} \right]. \end{aligned} \quad (8)$$

This completes the lattice definitions of the operators.

Before we proceed to evaluate them and extract the non-linear susceptibilities, we note an ambiguity that arises on the lattice due to the fact that there is no unique way of putting chemical potential on the lattice. One can associate a factor $f(a\mu)$ for the propagation of a quark forward in time by one lattice spacing and a factor $g(a\mu)$ for the propagation of an antiquark. There are exactly four physical conditions that these two functions must satisfy

[15]. In the absence of chemical potential the usual lattice theory must be recovered, hence $f(0) = g(0) = 1$. CP symmetry gives $f(-a\mu) = g(a\mu)$. Finiteness of the energy density is guaranteed if $f(a\mu)g(a\mu) = 1$. Finally, the correct continuum limit requires $f'(0) = 1$. These constraints imply the further relations, $f''(0) = 1$ and $f^{(n)}(0) = (-1)^n g^{(n)}(0)$, where the superscript n on f and g denotes the n -th derivative. All this guarantees that n_f and χ_{fg} are prescription independent.

The four conditions above also give relations between the remaining $f^{(n)}$, such as $f^{(4)} = 4f^{(3)} - 3$, but do not fix their numerical values. Since μ appears linearly in the continuum Lagrangian, these higher derivatives are all lattice artifacts. Any extra conditions imposed to fix them cannot be physical, and must remain at the level of prescription. The usual prescription, $f(a\mu) = \exp(a\mu)$ [16], which we call the HK prescription, gives $f^{(n)}(0) = 1$, but the alternative BG prescription $f(a\mu) = (1 + a\mu)/\sqrt{(1 - a^2\mu^2)}$ [17] gives $f^{(3)}(0) = 3$ and $f^{(4)}(0) = 9$.

The difference between the two prescriptions can be rather significant. At any fixed cutoff, one may try to roughly map two prescriptions on to each other by changing μ while holding Z fixed by keeping $f(a\mu)$ unchanged. This gives the relation that for constant physics we must have

$$a\mu_{BG} = \tanh(a\mu_{HK}), \quad (9)$$

where this mapping is for quark chemical potentials. On $N_t = 4$ lattices, the critical endpoint for 2+1 flavour QCD has been determined to be at $T_E = 160 \pm 3.5$ MeV and $\mu_E^{HK} = 725 \pm 3$ MeV [1]. The matching formula of eq. (9) then shows that $\mu_E^{BG} \simeq 692$ MeV, and hence the resultant uncertainty in μ_E from this source alone is about 11 times larger than the statistical errors. We next show that this ambiguity vanishes in the continuum limit in all prescriptions. We also show later (Table II) that uncertainties of almost 20% are also expected from other finite lattice spacing effects even within one prescription, and lattice spacings of $1/12T_E$ may be required to find μ_E stable within statistical error bars.

This freedom of choosing a prescription has specific consequences for the third and higher derivatives of M , and through them for the non-linear susceptibilities, and hence for F , P and all quantities at finite μ and a . At $\mu_f = 0$, the derivatives of M are related by

$$M^{(n)} = f^{(n)} a^{n-2} M' \quad (n \text{ odd}) \quad M^{(n)} = f^{(n)} a^{n-2} M'' \quad (n \text{ even}). \quad (10)$$

As a result, $\mathcal{O}_3 = \mathcal{O}_3^{HK} + \Delta f^{(3)} a^2 \mathcal{O}_1$ and $\mathcal{O}_4 = \mathcal{O}_4^{HK} + 4\Delta f^{(3)} a^2 \mathcal{O}_2$, where the superscript

HK on an operator denotes its value obtained in the HK prescription and $\Delta f^{(3)} = f^{(3)} - 1$. Clearly, the prescription dependence, manifested as a non-vanishing $\Delta f^{(3)}$ at this order, disappears in the continuum limit, $a \rightarrow 0$. Since $\langle \mathcal{O}_1 \rangle = 0$ at $\mu = 0$, the prescription dependence of $\langle \mathcal{O}_3 \rangle$ is invisible. We find that $\chi_{uuud} = \chi_{uuud}^{HK} + \Delta f^{(3)}(\chi_{ud}/T^2)/N_t^2$. Since χ_{ud} vanishes within errors, as we show later, χ_{uuud} turns out to be effectively prescription independent. From the relation for \mathcal{O}_4 we find, on varying N_t at fixed T ,

$$\chi_{uuuu} = \chi_{uuuu}^{HK} + \Delta f^{(3)} \left(\frac{\chi_{uu}}{T^2} \right) \left(\frac{4}{N_t^2} \right). \quad (11)$$

Finally, χ_{uudd} involves neither $M^{(3)}$ nor $M^{(4)}$, and hence is prescription independent. The prescription dependence of other susceptibilities can be systematically worked out, and it can be shown exactly as above that they become physical only in the continuum. Mixed derivatives of T and μ also have similar behaviour. If the dependence on a of each susceptibility were known in any scheme, then one could write down an improved prescription by removing finite a effects systematically. In other schemes every quantity is potentially prescription dependent at finite lattice spacing.

After this analysis of lattice artifacts in the Taylor coefficients, we return to the Taylor expansion itself. Along the line $\mu_u = \mu_d = \mu$, the Taylor series expansion of P can be written in the form

$$\frac{\Delta P}{T^4} = \left(\frac{\chi_{uu}}{T^2} \right) \left(\frac{\mu}{T} \right)^2 \left[1 + \left(\frac{\mu/T}{\mu_*/T} \right)^2 + \mathcal{O} \left(\frac{\mu^4}{\mu_*^4} \right) \right], \quad (12)$$

where $\Delta P = P(\mu) - P(\mu = 0)$, we have neglected χ_{uudd} in anticipation of our numerical results (Tables I and II), and

$$\frac{\mu_*}{T} = \sqrt{\frac{12\chi_{uu}/T^2}{|\chi_{uuuu}|}}. \quad (13)$$

For an ideal gas in the continuum, $\chi_{uu}/T^2 = 1$ and $\chi_{uuuu} = 6/\pi^2$, giving $\mu_*/T = \sqrt{2}\pi \simeq 4.43$. Some remarks are in order—

1. The series within square brackets in eq. (12) is prescription dependent at any non-zero lattice spacing, and hence physical values of ΔP can be most reliably extracted by extrapolating each term in the series to the continuum.
2. For those values of μ at which the second or higher order terms in the brackets in eq. (12) are important, computations of $\Delta P/T^4$ on lattices with finite N_t are necessarily prescription dependent. Since $F = -PV$, the same is evidently true for all other

T/T_c	m_V/T	$10^6 \chi_{ud}/T^2$	$10^6 \chi_{uuud}$	$10^4 \chi_{uudd}$	μ_*^{HK}/T
1.0	0.2	6 (30)	4 (17)	7 (1)	3.20 (3)
	0.1	8 (42)	7 (33)	9 (2)	3.31 (5)
	0.03	11 (84)	20 (172)	11 (2)	3.38 (4)
1.5	0.2	-0.3 (423)	-0.7 (116)	0.107 (3)	3.73 (1)
	0.1	0.6 (431)	-0.6 (128)	0.105 (3)	3.84 (1)
	0.03	-0.07 (433)	-0.5 (166)	0.106 (3)	3.86 (2)
2.0	0.2	2 (36)	0.5 (85)	0.097 (3)	3.83 (1)
	0.1	2 (36)	0.5 (89)	0.098 (3)	3.87 (1)
	0.03	1 (35)	0.6 (82)	0.096 (3)	3.78 (2)
3.0	0.2	0.6 (19)	0.1 (5)	0.032 (2)	3.87 (1)
	0.1	0.6 (20)	0.1 (5)	0.033 (2)	3.88 (2)
	0.03	0.6 (20)	0.1 (5)	0.033 (2)	3.88 (2)

TABLE I: Results in two flavour QCD with sea quark $m/T_c = 0.1$. For $T = T_c$ the results are based on 2017 configurations, for $1.5T_c$ on 370, for $2T_c$ on 126 and for $3T_c$ on 60. At T_c and $3T_c$ 100 noise vectors were used. χ_{uuuu} can be extracted from μ_* and χ_{uu} using eq. (13).

physical quantities, including the energy density. From eqs. (11 and 13), it is clear that the prescription dependence of the quadratic term is $(\mu_*/T)^2/3N_t^2$. For $N_t = 4$ this can be as large as 33% (see Table II).

3. If the series in eq. (12) is well behaved, *i.e.*, sixth and higher order susceptibilities are not much larger than χ_{uuuu} , then this expansion must be well approximated by the leading term for $\mu \ll \mu_*$ in every prescription, and hence be effectively independent of prescription [18]. Other finite lattice spacing effects may still exist.
4. The series expansion must fail to converge in the vicinity of a phase transition; therefore estimates of (T_E, μ_E) on finite lattices must be prescription dependent, as we have already estimated. Computation of the continuum limit of several terms in the double series for $F(T, \mu)$ may allow us to use series extrapolation methods, such as Padé approximants or estimates of radius of convergence [19], to identify (T_E, μ_E) in the continuum limit.

T/T_c	N_t	$10^6 \chi_{ud}/T^2$	$10^6 \chi_{uuud}$	χ_{uuuu}	μ_*^{HK}/T
1.5	4	2 (28)	-0.7 (56)	1.48 (2)	3.81 (2)
	8	0.2 (15)	0.2 (13)	0.70 (1)	4.36 (4)
	10	-0.4 (77)	0.04 (64)	0.61 (2)	4.47 (4)
	12	-0.5 (5)	0.00 (30)	0.56 (1)	4.55 (4)
	14	0.9 (58)	0.00 (24)	0.53 (1)	4.56 (4)
	∞	—	—	0.45 (1)	4.67 (4)
2.0	6	0.2 (67)	0.2 (10)	1.01 (1)	4.11 (1)
	8	-0.3 (115)	0.1 (13)	0.74 (1)	4.32 (5)
	10	-0.3 (76)	0.007 (49)	6.37 (3)	4.45 (3)
	12	0.0 (57)	0.00 (34)	0.58 (1)	4.56 (3)
	14	-0.2 (43)	0.00 (17)	0.56 (1)	4.59 (4)
	∞	—	—	0.49 (3)	4.76 (4)
3.0	4	2 (25)	0.8 (44)	1.54 (1)	3.85 (1)
	8	2 (4)	0.1 (4)	0.79 (2)	4.25 (5)
	10	-0.6 (14)	-0.04 (11)	0.66 (1)	4.40 (3)
	12	-0.1 (17)	-0.02 (7)	0.61 (1)	4.48 (4)
	14	-0.2 (8)	0.00 (3)	0.58 (1)	4.51 (2)
	∞	—	—	0.496 (1)	4.62 (1)

TABLE II: Results in quenched QCD with $m_v/T_c = 0.1$. Quadratic extrapolations to the continuum limit, $N_t = \infty$, from the last three points, are shown. μ_* and χ_{uuuu} are related by eq. (13).

We turn now to our numerical simulations. For dynamical sea quark mass $m/T_c = 0.1$ we studied the higher order susceptibilities at $T = T_c$ on a 4×10^3 lattice, $1.5T_c$ and $2T_c$ on 4×12^3 lattices, and $3T_c$ on a 4×14^3 lattice. All the simulations were performed using the hybrid R-algorithm [20] with molecular dynamics trajectories integrated over one unit of MD time using a leap-frog algorithm with time step of 0.01 units. At T_c autocorrelations of the Wilson line and the quark condensate were found to be between 150 and 250 trajectories. With over 2000 saved configurations separated by 10 trajectories each, this gave the equivalent

of about 100 independent configurations. For $T > T_c$ the autocorrelations were all less than 10 trajectories, and hence all the saved configurations can be considered statistically independent.

Quark number susceptibilities were evaluated in the HK prescription on stored configurations using valence quark masses $m_V/T_c = 0.2, 0.1$ and 0.03 . The smallest valence quark mass is chosen such that the ratio of the ($T = 0$) rho and pion masses reaches its physical value 0.2 at the lattice spacing $a = 1/4T_c$. All quark-line disconnected diagrams of the kind needed for these measurements are evaluated using a straightforward extension of the stochastic method given for χ_{ud} in [21] using 10 to 100 noise vectors per configuration [22]. Our results for the non-linear susceptibilities which do not vanish by symmetry are shown in Table I. It is clear that of these only χ_{uudd} and χ_{uuuu} , are non-zero with statistical significance. Comparing them to computations with sea quark mass $m/T_c = 0.2$ and various volumes, we concluded that they are free of sea quark mass and finite volume effects. Also note the stability in physical quantities as m_v/T_c decreases from 0.1 to 0.03 .

With present day computer resources the continuum limit is hard to take in QCD with dynamical quarks. To investigate this limit we have evaluated the same quantities in quenched QCD for $T \geq 1.5T_c$ where the difference in the order of transitions is immaterial [23]. The run parameters are exactly as in [21]. Our results are shown in Table II. These results show that there is over 20% movement in μ_* when going from $N_t = 4$ to the continuum within a fixed prescription. Since μ_* is an estimate of the radius of convergence of the Taylor expansion at the fourth order, it implies that the estimate of the end-point, μ_E , may shift upward by about 20% due to finite size effects even inside the HK scheme. χ_{uudd} remains significantly non-zero on all the lattices, and there is some evidence that it becomes either zero or marginally negative in the continuum [24]. We shall present more detailed studies in the future. Finally, the results for $N_t = 4$ are very similar in the quenched and dynamical theories, leading us to believe that the continuum limits will also be close.

$\Delta P/T^4$ obtained in quenched QCD, using values of χ_{uu} from [21] and μ_*/T obtained here, are shown in Figure 2. At RHIC it is seen that $\mu/T_c = 0.06 \ll 0.15$, which implies that $\Delta P/T^4$ is negligible. In terms of dimensionless variables, the results in quenched and dynamical QCD are not expected to differ by more than 5–10% [25]. For $\mu/T_c \simeq 0.45$, relevant to SPS energies, the effects of $\mu > 0$ are more significant, but can still be reliably extracted using only the leading term of eq. (12). In this whole range of μ/T_c the results

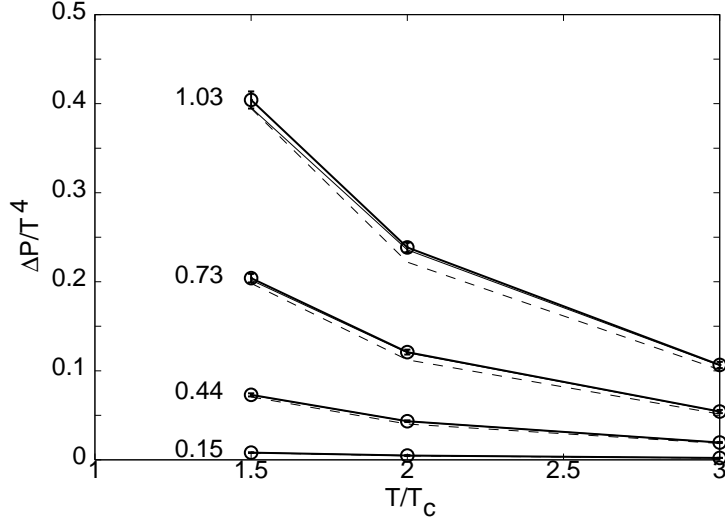


FIG. 2: $\Delta P/T^4$ as a function of T/T_c for the values of μ/T_c shown. Continuum results correct to $\mathcal{O}(\mu^4)$ (full lines) and $\mathcal{O}(\mu^2)$ (dotted lines) are shown. $N_t = 4$ results, in the HK prescription, correct to $\mathcal{O}(\mu^4)$ and multiplied by 0.47 to compensate for finite a effects in χ_{uu} are shown with dashed lines.

of [25], including a correction for finite lattice spacing artifacts in the evaluation of χ_{uu} at $N_t = 4$, are the same as our continuum results, and both are dominated by the leading term of eq. (12). Our computations show that for $\mu \geq 2T_c$, higher order terms become significant for the continuum limit. As a result, at these chemical potentials, reweighting on $N_t = 4$ lattices, even after correcting for finite a effects in χ_{uu} , are quite different from the continuum values.

In conclusion, we have studied non-linear susceptibilities and shown that they are prescription dependent at finite lattice spacing. We have found the continuum limit of these quantities in quenched QCD, and thereby removed these artifacts. This allows us to compute the finite chemical potential corrections to the pressure relevant to RHIC and SPS experiments. For $a = 1/4T$ the numerical results for QCD with and without dynamical quarks are similar, and we find the continuum limit of some of these quantities in the quenched theory. It would be interesting to compare them with perturbation theory. We have argued that the critical end point (T_E, μ_E) evaluated at $N_t = 4$ is uncertain by more than 10 times the statistical errors. As a result, a continuum extrapolation is required to obtain the physical value of the end point. This may be possible with the computation of several non-linear

susceptibilities.

We would like to thank J.-P. Blaizot for discussions.

APPENDIX A: LATTICE OPERATORS

In this appendix we work in lattice units, *i.e.*, we choose the lattice spacing to be unity. We introduce the compact notation

$$\text{Tr} \left[\left(M^{-1} M^{(p_1)} \right)^{n_1} \left(M^{-1} M^{(p_2)} \right)^{n_2} \cdots \right] = (n_1 \cdot p_1 \oplus n_2 \cdot p_2 \oplus \cdots), \quad (\text{A1})$$

and further write $(1 \cdot p)$ as (p) . Since the trace allows only cyclic permutations, therefore

$$(a \oplus b \oplus c) = (c \oplus a \oplus b) \neq (b \oplus a \oplus c), \quad (\text{A2})$$

i.e., the ‘addition’ (represented by \oplus) is not commutative. ‘Multiplication’ (denoted by the dot) is distributive over addition, subject to restrictions due to non-commutativity, *i.e.*,

$$\begin{aligned} (n \cdot p \oplus m \cdot p) &= ((n + m) \cdot p), \\ (n \cdot p \oplus m \cdot p' \oplus l \cdot p) &= ((n + l) \cdot p \oplus m \cdot p'), \end{aligned} \quad (\text{A3})$$

but no simplification is possible for $(n \cdot p \oplus m \cdot p' \oplus l \cdot p \oplus \cdots)$. Traces can be added, *i.e.*,

$$a(n \cdot p) + b(n \cdot p) = (a + b)(n \cdot p). \quad (\text{A4})$$

The point of all this is to simplify the taking of derivatives. These are easy to write—

$$(n \cdot p)' = -n(1 \oplus n \cdot p) + n((n - 1) \cdot p \oplus (p + 1)). \quad (\text{A5})$$

The operation of taking derivatives is linear over the ‘addition’ \oplus , since this is just the rule for taking derivatives of products.

We have the first examples

$$\emptyset_1 = (1), \quad \emptyset_2 = -(2 \cdot 1) + (2). \quad (\text{A6})$$

Then, the remaining known ones are obtained simply by applying the rules again. Since $(2 \cdot 1)' = -2(3 \cdot 1) + 2(1 \oplus 2)$ and $(2)' = -(1 \oplus 2) + (3)$, we first obtain the relation in eq. (8),

$$\emptyset_3 = 2(3 \cdot 1) - 3(1 \oplus 2) + (3). \quad (\text{A7})$$

At the fourth order we need the derivatives

$$\begin{aligned}
(3 \cdot 1)' &= -3(4 \cdot 1) + 3(2 \cdot 1 \oplus 2), \\
(1 \oplus 2)' &= -2(2 \cdot 1 \oplus 2) + (2 \cdot 2) + (1 \oplus 3), \\
(3)' &= -(1 \oplus 3) + (4).
\end{aligned}
\tag{A8}$$

As a consequence of the general rule in eq. (A5), the coefficients sum up to zero. This is a consequence of the rule for derivatives in eq. (A5). Also note that each operator, $(\dots \oplus n_i \cdot p_i \oplus \dots)$, which contributes to \mathcal{O}_n must satisfy the constraint $\sum n_i p_i = n$. The expressions in eq. (A8) give the result of eq. (8),

$$\mathcal{O}_4 = -6(4 \cdot 1) + 12(2 \cdot 1 \oplus 2) - 3(2 \cdot 2) - 4(1 \oplus 3) + (4).
\tag{A9}$$

For each \mathcal{O}_n for $n \geq 2$, the sum of the coefficients is zero, as can be proved by induction from eq. (A5).

Using these rules higher order derivatives, needed for the higher order susceptibilities, can be easily written down. Since these manipulations are simple rules for rewriting expressions, not only are they easy to automate inside standard algebra packages, but can even be readily implemented as macros in text editors such as sed or emacs.

-
- [1] Z. Fodor and S. D. Katz, *J. H. E. P.*, 03 (2002) 014.
 - [2] C. R. Allton *et al.*, *Phys. Rev.*, D 66 (2002) 074507.
 - [3] M. D'Elia and M.-P. Lombardo, hep-lat/0209146.
 - [4] P. De Forcrand and O. Philipsen, *Nucl. Phys.*, B642 (2002) 290.
 - [5] J. Cleymans, *J. Phys.*, G 28 (2002) 1575.
 - [6] See, for example, U. Heinz, nucl-th/0212004.
 - [7] S. Gupta, hep-lat/0301006.
 - [8] T_c stands for the crossover temperature in 2 flavour QCD with finite mass quarks, and the critical temperature in quenched QCD.
 - [9] Z is, of course, real and positive even for $\mu > 0$. In the quenched theory valence quarks exist and μ acts on them.

- [10] The determinant for each flavour is obtained as usual by taking the fourth root of each staggered quark determinant. As a result, there is a factor $1/4$ for each quark loop evaluated with staggered quarks.
- [11] At vanishing μ , the effects of breaking the vector part of the flavour symmetry are small; see R. V. Gvai and S. Gupta, *Phys. Rev.*, D 66 (2002) 094510.
- [12] S. Gottlieb *et al.*, *Phys. Rev. Lett.* 59 (1987) 2247.
- [13] The derivatives of Z are called moments, and those of $\log Z$ are called cumulants, and relations between them can be found in any standard textbook on probability. See for example, J. G. Kalbfleisch, *Probability and Statistical Inference*, Vol I (Probability), Springer Verlag, New York, 1985.
- [14] S. Gupta, *Acta Phys. Pol.*, B 33 (2002) 4259.
- [15] R. V. Gvai, *Phys. Rev. D* 32 (1985) 519.
- [16] P. Hasenfratz and F. Karsch, *Phys. Lett.*, B 125 (1983) 308.
- [17] N. Bilic and R. V. Gvai, *Z. Phys.*, C 23 (1984) 77.
- [18] Interestingly, at finite isospin density ($\mu_u = -\mu_d = \mu_3/2$) the expression for $\Delta P/T^4$ is also given by eq. (12). For imaginary μ_B , $\Delta P/T^4$ is negative and the higher order terms in eq. (12) alternate in sign.
- [19] See for example, C. Domb and M. S. Green, *Phase Transitions and Critical Phenomena*, Vol III, Academic Press, London, 1974.
- [20] S. Gottlieb *et al.*, *Phys. Rev.*, D 35 (1987) 2531.
- [21] R. V. Gvai and S. Gupta, *Phys. Rev. D* 67 (2003) 034501.
- [22] Our results are stable under change of such algorithmic parameters.
- [23] R. V. Gvai, S. Gupta and P. Majumdar, *Phys. Rev. D* 65 (2002) 054506.
- [24] A perturbative estimate of χ_{uudd} can be obtained from J.-P. Blaizot *et al.*, *Phys. Lett.*, B 523 (2001) 143, and suggests a value $\mathcal{O}(10^{-3})$, in excess of the lattice results. Recent estimates from a dimensionally reduced theory agree with them (A. Vuorinen, hep-ph/0305183).
- [25] See also, Z. Fodor *et al.*, hep-lat/0208078.